Development of a stacked wire-mesh structure for diesel soot combustion

CrossMark

Ezequiel D. Banús [a], Oihane Sanz [b,*], Viviana G. Milt [a], Eduardo E. Miró [a], Mario Montes [b]

[a] Instituto de Investigaciones en Catálisis y Petroquímica (INCAPE, FIQ, UNL-CONICET), Santiago del Estero 2829, 3000 Santa Fe, Argentina
[b] Dept. of Applied Chemistry, UFI 11/56, Chemistry Faculty, University of the Basque Country, UPV/EHU, Pº Lardizabal, 3, 20018 San Sebastian, Spain

HIGHLIGHTS

- New catalytic wire-mesh filters for diesel soot combustion.
- Metallic filters designed and built using wire-mesh discs of AISI 304.
- Excellent Co, Ba, K/CeO$_2$ catalyst washcoating.
- Wire-mesh geometry influences directly the coating adhesion of the catalyst.
- Very high activity at temperatures relevant for diesel soot abatement.

GRAPHICAL ABSTRACT

Catalytic diesel soot filter made of wascoated wire meshes.
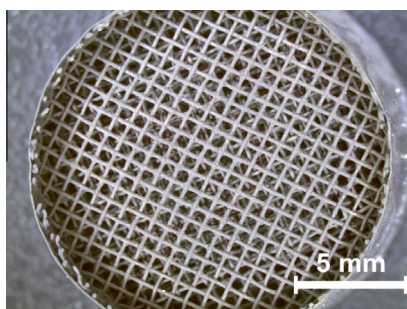
5 mm

ARTICLE INFO

ABSTRACT

This work describes the development of stacked wire-mesh structures and their washcoating method to prepare a structured system for the catalytic combustion of soot. For this purpose, a metallic structured substrate was designed and built using wire-mesh discs of AISI 304. The coating of this substrate was optimized by investigating various strategies and parameters of the washcoating such as the suspension formulation (sol–gel coating with posterior impregnation of the active phase, the all-in-one strategy using catalyst precursors and the preparation of the catalyst slurry with a ready-made catalyst), the amount of Co, Ba, K/CeO$_2$ catalyst and the packing material (wire diameter and number of packed discs). The coating proposed strategies were analyzed measuring textural properties, catalyst coating adherence and morphology, and pressure drop of the catalytic substrate. Finally, the coated wire-mesh substrates were tested in the combustion of soot showing promising catalytic activity.

1. Introduction

Diesel engines emit nitrogen oxides and soot that are produced during the fuel combustion [1]. Since both pollutants have negative environmental effects, research in this field has received increasing consideration in the last decades.

Many options for the catalytic removal of soot from diesel exhaust gases have been considered. The powder catalyst itself cannot be used for a practical application in the diesel engine exhaust pipe due to the severe operating conditions of the high flows. Therefore, the catalytic filters coated with a catalytic layer are considered an attractive system. These structure substrates with filtration properties trap the soot particles and allow their burning at the exhaust gases temperature [2,3].

The most popular way to trap diesel particles is by means of surface filtration, sometimes known as a cake filtration or sieving [4], using monoliths made of cordierite [3–6] or silicon carbide [7,8]. These structures can be used as particulate filters when

channels are alternatively plugged to force the diesel exhaust to flow through the porous walls of the monoliths and, in this way, soot particles are trapped. The wall-flow monolith filter acts as a cake filter, i.e. after some initial particle deposition into the pores of the monolith walls occurs, the cake layer formed becomes the dominant filtration medium [4,9]. But, in general, these monoliths offer significant pressure drop and narrow channel structures inside which a laminar flow takes place, and this fact implies mass-transfer limitation from the gas phase to the catalytic layer on the wall.

A second possibility is to use deep-bed filters using materials of relatively open structure compared to surface filters. In these filters, soot is retained throughout the filter structure by three well-known mechanisms: Inertial interception, Brownian diffusion and flow-line interception [4]. The main advantage of this strategy is the much better contact between the deposited soot and the catalyst coating of the filter, making it easier to regenerate the filter continuously. Deep-bed filters can be made of foams [9,10] or wire-meshes [11]. These substrates can be used in multifunctional reactors, which combine reaction and separation (filtration, adsorption), or combustion of feed mixtures containing gaseous and organic matter as particulates (soot) in a layered reactor [9,12,13]. During the last years foams and wire-meshes have not been considered as good filters [4]. However, Vanhaecke et al. [9] recently published that a β-SiC foam with pore diameter (window size) of 500 ± 25 μm was effective in filtering ultrafine soot particles checked in a real bench test. Doggali et al. [13] also suggested that ceramic foams present especially potential option for old generation engines with very high PM emissions. Moreover, the efficiency of wire-mesh filters with window sizes similar to that of foams would be relatively low at the beginning, but during the particle deposition it would increase [14]. On the other hand, as Van Setten et al. [4] pointed out, the reported efficiencies are reasonable, especially when one considers that non optimized materials are used (standard foams are designed for other applications such as molten-metal filtration or structural material). Higher filtration efficiencies might be expected for tailor-made materials, among them wire-meshes, which can be found in many commercial sizes of wire and mesh openings.

In spite of the fact that there are few studies about wire-meshes for soot combustion, these filters present interesting properties to be used as substrates. The most attractive feature of the wire-mesh substrate is the price: the cost of these structured substrates is only about 25% that of ceramic honeycombs and foams [15]. There have been attempts to utilize wire-meshes made of cheap iron or stainless steel as supports for active catalyst component [16–18]. In addition, wire-mesh catalysts combine the excellent mass- and heat-transfer characteristics of pellets catalysts with a relatively low pressure-drop monolith, which is mainly attributed to the high porosity of the wire-mesh structures [12]. The radial mixing of the gases flow can readily occur through porous mesh structures yielding a more uniform distribution of fluids across the entire bed diameter [15]. Another advantage of the fibrous catalyst is its easy scale-up. The geometric flexibility of the wire-mesh catalyst makes it suitable for retrofit installations. It is thus possible to adapt the geometric appearance of the wire-mesh catalyst to almost any form required.

Numerous literature reports on the performance of wire-mesh catalysts study the influence of many design variables such as supporting grids, wire diameter, packing density, construction geometry (for honeycomb [17,18], rolling sheet [16] or packaged sheets [19]) and construction material (steel [16], nickel [20] or precious metals [21]). In order to prepare catalysts based on metallic wire-mesh, it is necessary to solve the problem of deposition of the catalytic layer (oxide support + active phase) over the metal wire. Since the thermal expansion coefficient of the metallic structured substrate is different from the oxide support coating, the major problem is how to achieve a better adherence to the surface of the wire-mesh substrate. Various methods for obtaining well-adhered coatings on metallic substrates have been developed, including chemical vapor deposition (CVD), plasma spraying, washcoating and electrophoretic deposition [22,23]. But the preferred method for coating the oxide support powder is usually the conventional washcoating method, in which a fine thickness of catalyst support layer is formed on the surface of metallic substrate by repeatedly dipping the substrate into a slurry containing particles of the catalyst support materials, followed by drying and calcining. However, the authors that used washcoating methods for coating fibrous materials observed poor adherence and non-uniformity of the resulting coating [24,25]. Moreover, the coatings may flake away under the influence of mechanical stress [15]. On the other hand, few results have been reported about the coating adherence to wire-meshes using other coating methods. Ahlström-Silversand and Ingemar-Odenbrand [11] showed improved adherence of Al_2O_3 layers by the spray-deposition method, but other authors selected electrophoretic deposition of the Al_2O_3 layer as a pretreatment of the metallic wire mesh to generate a rough interlayer between wire-mesh surface and catalyst coating [17,20,26]. Nevertheless, this interlayer on wire-mesh is unnecessary when the catalyst is deposited by in situ growing [16,27] or using expensive metallic wire meshes that are active for the studied reaction [20,21].

For the ultimate goal of developing systems for the removal of diesel soot using wire-meshes, two major tasks must be addressed. One is the optimization of the filtering properties of the structure and the other, the effectiveness of the deposition of the catalyst active for the diesel soot oxidation on the wire meshes. This work focuses on the second one, where different strategies of coating are studied, along with the characterization of the produced structured catalysts and their catalytic properties for the oxidation of diesel soot.
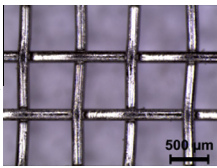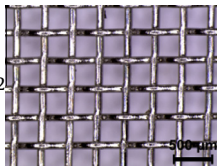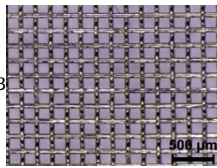
2. Experimental

2.1. Construction of the wire-mesh structured substrate

Different wire-mesh discs of AISI 304 stainless steel (Filtra Vibración S.L.) were used in this work. The main characteristics of these wire-meshes are presented in Table 1. Fig. 1 shows the stages of construction of the structured substrate. The first stage was the building of a spot-welded cylindrical cartridge of AISI 304 stainless steel (50 μm thickness, Goodfellow) of 16 mm in diameter and a height that depended on the number of wire-mesh discs of the structure (5–40 discs, which resulted in substrates 6–30 mm in height).

The wire-meshes were cut and corrugated (Fig. 1) in a home-made embossing tool (Fig. 1a), in this way allowing discs to remain slightly separated when stacked. Corrugated discs were 90° alternately stacked to prevent intermeshing within the metallic cartridge (Fig. 1d) and two mesh covers were also spot welded to lock the assembly (Fig. 1e). The substrate was then washed first in detergent–water and then in methanol, during 30 min in each solvent, in an ultrasonic bath.

Given its simplicity and versatility, the washcoating method was chosen to deposit the catalyst onto the structured supports. The pre-treatment of the metallic substrate before washcoating was necessary because the anchoring and interlocking of the washcoat particles with the surface irregularities produced in the pre-treated metallic substrate played an important role on the adherence of the catalyst to the structured substrate [28,29]. As reported, most of the coated metallic wire-meshes prepared without pre-treatment showed poor adherence [20,24,25]. Yang et al. [20]

Table 1
Geometric characteristics of the investigated meshes.

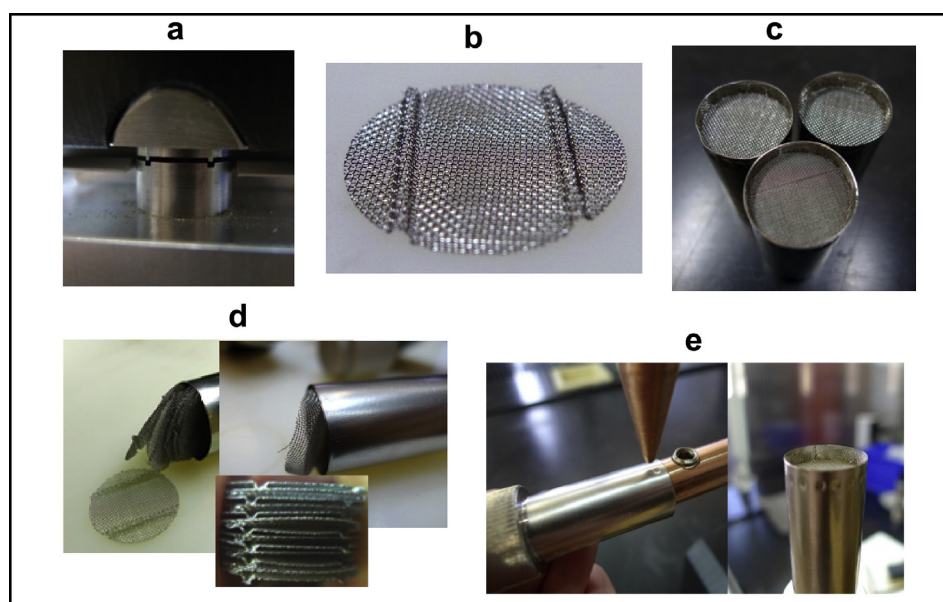| Wire-mesh characteristics	WM1	WM2	WM3
Wire diameter (μm)	160	100	60
Mesh opening (μm)	530	250	125
Geometric surface area (cm^2/g)	32	50	84
Frontal open area (%)	59	51	46

Fig. 1. Stages of the wire-mesh structured substrate construction. (a) Detail of the cutter and the bender of the wire-mesh disc, (b) wire-mesh disc, (c) detail of the cover of the monolith with the top spot welded to the cylindrical cartridge of AISI 304 stainless steel, (d) detail of the insertion of the wire-mesh disc, arrangement in the cylindrical cartridge of AISI 304 stainless steel, and colocation of the cover and (e) welding and closed monolith of stacked wire meshes.

observed that there was a main drawback for using an untreated stainless steel wire-mesh as substrate, since TiO$_2$ coating deposited by electrophoretic deposition produced a cracked coating due to the differences in the thermal expansion coefficients of titania and stainless steel. In this way, our experience in coating monoliths and foams made of AISI 304 stainless steel showed that a metallic surface thermally heated in air produced a rough layer that enhanced the adherence of the catalytic coating [30,31]. The wire-mesh structured substrates were calcined at 900 °C for 1 h in a tubular furnace in atmosphere of synthetic air (10 ml/min, heating rate 10 °C/min). The oxide layer generated during the calcination also protects the metallic structured substrate [30,31]. The structured substrate thus prepared and pre-treated was washcoated with the catalytic components, as described below.

2.2. Strategies for coating

The technique used for coating the wire-mesh structured substrate was either dip coating or washcoating. The external surface of the substrates was previously covered with a masking tape to produce the catalyst coating exclusively on the metal mesh and the internal surface of the cartridge. The velocity of immersion and emersion was 3 cm/min. In a first stage, the parameters of the elimination of the suspension excess by centrifugation were studied. Two methods were studied for the drying of the

structures, one using static air and the other using air flowing and in both cases, the temperature was 120 °C. The catalyst load is expressed as specific load, i.e., mg of catalyst per cm^2 of substrate using the geometric surface area data presented in Table 1.

The Co, Ba, K/CeO$_2$ catalyst was selected to be deposited on a wire-mesh substrate because of the excellent activity shown in diesel soot combustion [32]. Three strategies were explored to obtain the catalytic coating on the wire-meshes. The first one was a sol–gel coating with colloidal ceria (suspension 1), a subsequent step being necessary to introduce the active components (active phase). The second one was the all-in-one strategy using suspension 2 that contained the catalytic support and all the precursors of the active phase in an attempt to simultaneously produce the catalyst and the coating. The last one consisted in using suspension 3 prepared with the previously synthesized catalyst.

2.2.1. Suspension 1

The sol–gel coating of the wire-mesh structured substrate was carried out with a commercial colloidal suspension of CeO$_2$ (Nyacol®, 20 wt./wt.%, $d_{particle}$ = 10–20 nm), which was used as received or with the addition of 5 wt./wt.% polyvinyl alcohol (PVA, Sigma Aldrich), denoted as suspension 1A and suspension 1B, respectively. The subsequent introduction of the active phase by impregnation was discontinued because this strategy needed

both too many immersions to load the desired amount of catalyst and an additional step of active phase impregnation.

2.2.2. Suspension 2

This suspension contained all the precursors for the catalyst preparation: CeO_2 Nyacol®, as the source of CeO_2, barium acetate, cobalt acetate and potassium nitrate (Sigma Aldrich), as sources of Ba, Co and K, respectively. PVA was also added for modifying the suspension properties. The mass ratio between the components (H_2O:PVA:KNO_3:Co($H_3C_2O_2$)$_2$:Ba($H_3C_2O_2$)$_2$:colloidal CeO_2) was 1:0.015:0.053:0.087:0.149:1.466, and the pH was adjusted to 3 by HNO_3 addition (the same pH of colloidal ceria).

2.2.3. Suspension 3

The powder Co, Ba, K/CeO_2 catalyst was prepared according to Milt et al. [32]. After calcination at 500 °C, it was ball milled during 30 min at 500 rpm, obtaining a particle size of $d_{[4.3]} = 2.3$ μm. Then, a suspension of the milled catalyst, PVA and CeO_2 (Nyacol®) in water was prepared, in a mass ratio of 0.317:0.029:0.356:1, respectively, and its pH was adjusted to 4 by HNO_3 addition. One important parameter in the preparation of a stable slurry is the Zeta potential of the solid. This variable indicates the pH range suitable to maximize the repulsion between particles and, consequently, improve the slurry stability [33]. The evolution of the Zeta potential as a function of the pH for the measured Co, Ba,K/CeO_2 catalyst showed that the isoelectric point of the catalyst was around pH 8, whereas at pH 4 the Zeta potential was relatively large (40 mV) and the catalytic particles were thus positively charged.

After coating the wire-meshes with any of the suspensions above described, the calcination was performed in a furnace during 2 h at 300 or 500 °C. In what follows, the structured catalysts will be designated according to Table 2, as aWMb_SUSPc/d, where a = is the number of stacked wire-mesh discs, b = the type of wire-mesh used, c = the type of suspension used to washcoat the catalytic components and d = the specific catalyst load (mg/cm^2).

2.3. Characterization

The Zeta Potential was measured using a MALVERN Zetasizer 2000 instrument. The solids were dispersed in an aqueous solution of NaCl 0.003 M. The pH of the solutions was adjusted with HNO_3 or NH_3 solutions. Particle size distribution of the catalyst was measured with a Laser Particle Size Analyzer MALVERN MasterSizer 2000. One hundred milligrams of solid were dispersed in 20 mL H_2O, the pH was adjusted to 4, and they were promptly submitted to ultrasound for 1 h before the measurement. The rheological

properties of the slurries were measured at 25 °C in a TA Rotational Viscosimeter AR 1500EX.

The adherence of the catalytic layer deposited onto the substrates was evaluated measuring the coating weight loss caused by the exposure of the sample to ultrasounds. The structured supports immersed in petroleum ether were submitted to an ultrasonic treatment for 30 min at room temperature [34]. After that, the samples were dried and calcined, and the weight loss was determined by the weight difference before and after the ultrasonic test. Results are presented in terms of the retained amount of coating on the structured substrate, expressed as percentage. This treatment was performed until no additional weight loss was detected, three cycles of 30 min being usually required.

The morphology of the surfaces during the different steps of the catalytic substrates preparation was observed by SEM (Hitachi S-2700). A Leica DFC280 optical microscope was also used and images were processed in a computer using the IM50 program of Leica. The textural properties of the structured supports and the powder catalyst were determined by nitrogen adsorption using a Micromeritics ASAP 2020 instrument using a homemade cell that allows analyzing the complete structured supports. The pressure drop of the wire-mesh structured substrate at different gas velocities was measured with a Digitron 2080P Pressure Meter.

X-ray diffractograms were obtained with a Shimadzu XD-D1 instrument with monochromator using Cu Kα radiation at a scan rate of 1 °/min, from $2\theta = 10–70°$. The software package of the equipment was used for phase identification. A Shimadzu IR Prestige-21 spectrometer was used to obtain the infrared spectra. Sample wafers were prepared by mixing the KBr powder with suspension 3, dried and calcined (ca. 1% sample in KBr). The spectra were acquired at 4 cm^{-1} resolution, accumulating 40 scans. A powder sample of suspension 3, dried and calcined, was used to get the LRS spectra in a Horiba JOBIN YVON LabRAM HR instrument. The excitation source was the 514.5 nm line of a Spectra 9000 Photometrics Ar ion laser with the laser power set at 30 mW.

2.4. Catalytic test

Different catalytic structures prepared with the suspension that produced the best coating results were evaluated in the catalytic combustion of soot. The performance of these catalysts was evaluated with different loaded amounts of soot, which were achieved from soot suspensions of either 600 or 3000 ppm of soot in n-hexane. To this aim, wire-mesh structures were dipped during one minute in the corresponding soot suspension to deposit soot on the wire-mesh surface, thus obtaining structures with low or high soot loadings. The objective is to achieve a loose soot-catalyst

Table 2
Adherences of the catalytic layers obtained with the different suspensions, number of wire-mesh discs of the structure, specific catalyst load and type of mesh.

Suspension	Viscosity (cP)	Structure reference	Number of discs	Type of wire-mesh	Specific catalyst load (mg/cm^2)	Adherence[a] (%) 300 °C	Adherence[a] (%) 500 °C
1A	11	5WM1_SUSP1A/2	5	1	2	26	–
1A		10WM1_SUSP 1A/2	10	1	2	50	–
1A		40WM1_SUSP 1A/2	40	1	2	70	–
1B	15	5WM1_SUSP 1B/2	5	1	2	50	–
1B		10WM1_SUSP 1B/2	10	1	2	65	–
1B		40WM1_ SUSP 1B/2	40	1	2	75	71
2	14	10WM1_SUSP 2/2	10	1	2	–	40
3		10WM1_SUSP 3/2	10	1	2	75	–
3		40WM1_SUSP 3/2	40	1	2	95	93
3		40WM1_SUSP 3/1	40	1	1	98	–
3	16	40WM1_SUSP 3/4	40	1	4	93	–
3		40WM2_SUSP 3/2	40	2	2	77	–
3		40WM3_SUSP 3/2	40	3	2	58	–

[a] Percentage of catalytic layer remaining adhered after the ultrasonic tests. The structured catalyst were calcinated at different temperature.

contact similar to that obtained under real conditions. However, it is clear that the laboratory method employed is not fully representative of the filtration dynamics in real diesel operation. Nevertheless, in agreement with other authors [35], we consider that it constitutes a good way to evaluate catalytic efficiencies under contact conditions representative of those obtained under real conditions.

The soot was obtained by burning commercial diesel fuel (Repsol–YPF, Argentina) in a glass vessel. After being collected from the vessel walls, the soot was dried in a stove at 120 °C for 24 h [36]. The performance of these catalysts under different reaction atmospheres was also evaluated. The reactor was fed with 20 ml/min of a mixture of NO and O_2 (balance, He). The concentration of NO was the same as the one used in previous studies [5,10] of 0.1% or 0, and the O_2 concentration was 18% or 5%. A Shimadzu GC-2014 Gas Chromatograph, with a Porapak Q column was used for the analysis of the gases.

3. Results and discussion

3.1. Influence of the preparation conditions on the coating morphology and stability

The AISI 304 stainless steel wire-mesh was thermally treated at 900 °C for 1 h, producing an average increase in weight of 0.20% due to the formation of an oxide layer of about 0.07 mg/cm^2 that is composed of a spinel structure $M'M_2O_4$ (M'= M = Mn, Fe, Cr). The homogeneous rough morphology of the resulting surface can be observed in Fig. 2, where spinel particles of about 0.6 μm can be observed. This layer has a strong adherence since any detectable detachment occurs after the 90 min of treatment in an ultrasonic bath.

After the wire-mesh substrate pretreatment, different washcoating conditions were used for coating the catalytic layers, as indicated in the Experimental section. Preliminary tests were carried out using structures with five discs of wire-mesh 1 (5WM1). In a first stage, it was observed that the coating conditions usually employed for monoliths with longitudinal channels were inappropriate in this case. For conventional cordierite monoliths, the elimination of the solids excess was achieved by blowing air through the channels, and the drying step was performed in an oven without forced air flow [22]. Under these conditions, the wire-mesh structures were partially plugged. In view of this result, the conditions of blowing and drying processes were modified, and the best results were obtained by eliminating the solids excess by centrifugation at 600 rpm during 5 min and drying during one hour in a hot air flow. With this new method, the results were excellent
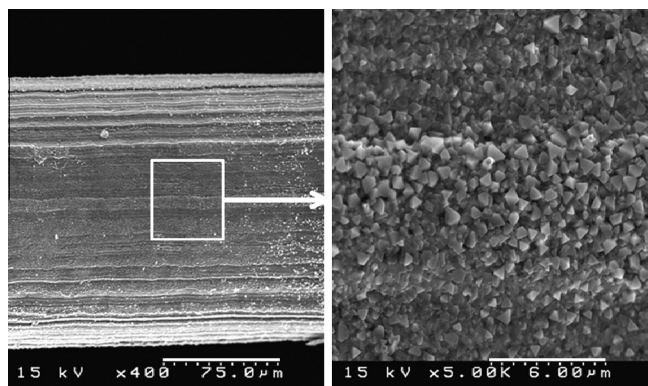

Fig. 2. SEM micrographs of the wire meshes after the thermal treatment at 900 °C for 1 h.
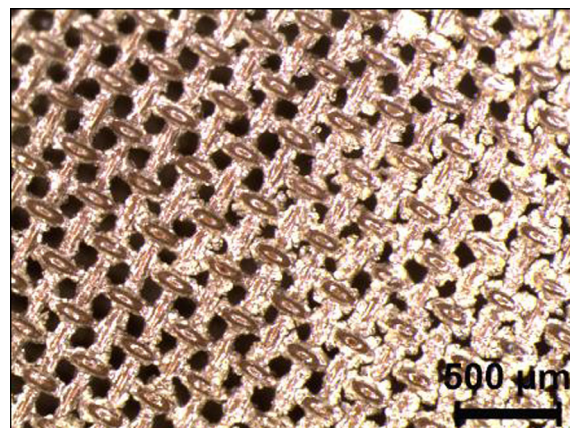

Fig. 3. Optical image of the wire-mesh structured substrate 3 (40WM3) coated with the best conditions of suspension elimination and drying.
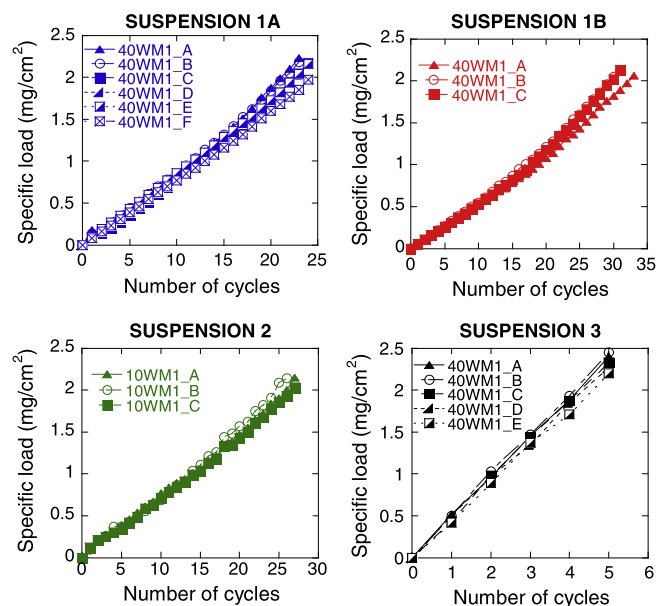

Fig. 4. Reproducibility of the specific catalyst load vs. coating cycles using different suspensions.
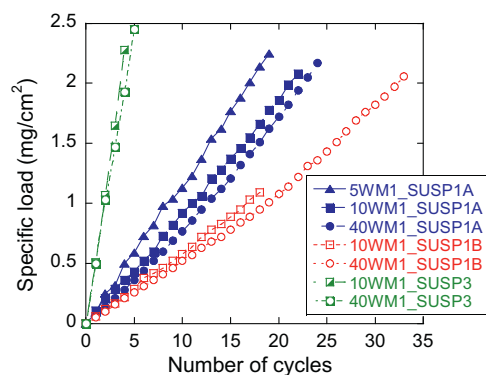

Fig. 5. Specific catalyst load vs. coating cycles for structures with different number of wire-mesh discs.

and only WM3 structures, which presented the narrower mesh opening, showed partial plugging for the highest specific catalyst load, as can be seen in Fig. 3.
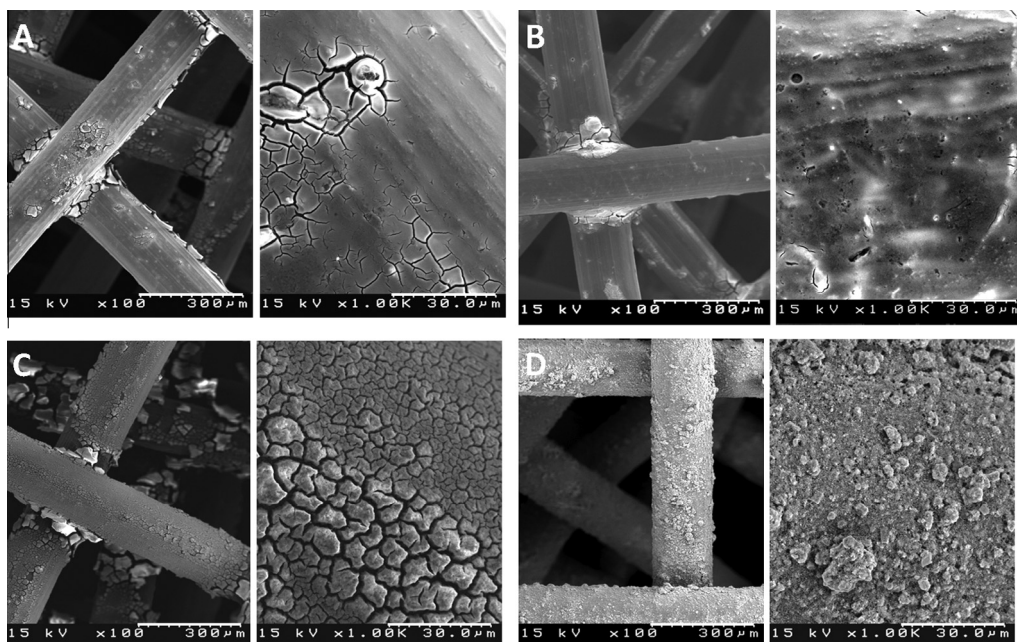
Fig. 6. SEM images of the catalytic layers obtained with the different suspensions before the adherence test: suspension 1A (A), suspension 1B (B), suspension 2 (C) and suspension 3 (D).
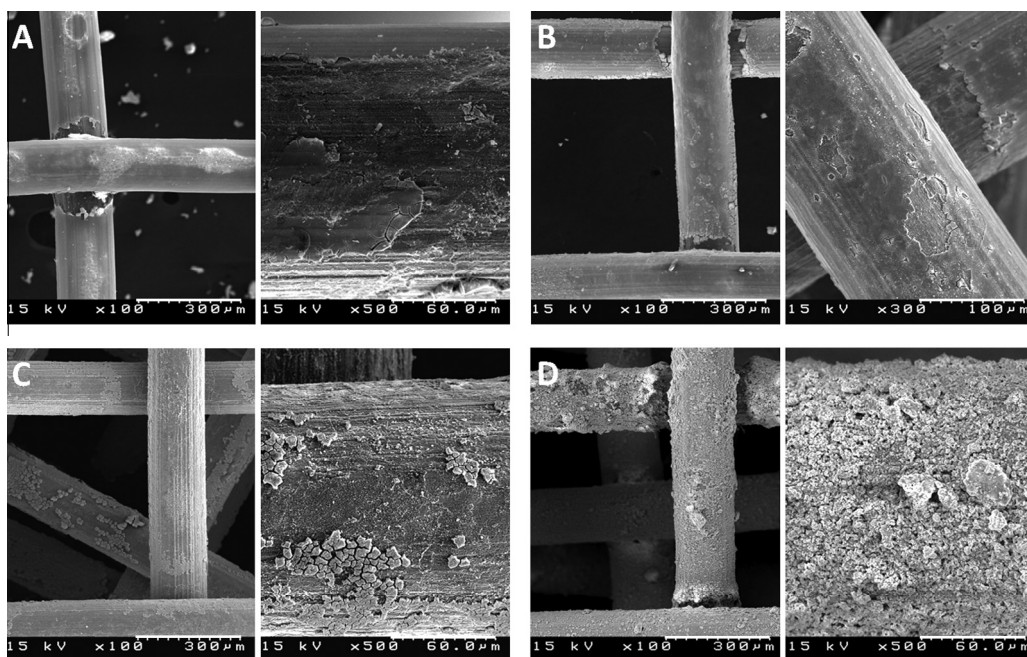

Fig. 7. Coating morphology of the catalytic structures (40WM1) obtained with the different suspensions after the adherence tests: suspension 1A (A), suspension 1B (B), suspension 2 (C) and suspension 3 (D).

Fig. 4 shows the reproducibility of the specific weight gains obtained for different suspensions. It can be observed that the reproducibility of the washcoating process in wire-meshes was excellent regardless of the suspension formulation used. On the other hand, the number of immersion steps needed to load 2 mg/cm^2 depended on the suspension used. The suspension prepared with the previously synthesized catalyst (suspension 3) allowed loading 2 mg/cm^2 with five to six times fewer coatings.

The effect of the number of packaged wire-mesh discs was also studied. Fig. 5 shows the specific load obtained when using different suspensions. It can be clearly observed that the number of wire-mesh discs influenced the specific weight gain. These differences were more important when changing from 5 to 10 discs, than from 10 to 40 discs. For structured substrates with 5, 10 and 40 discs the specific weight loaded in each immersion with suspension 1A were 0.118, 0.093 and 0.090 mg/cm^2, respectively. Small differences in specific weight in each immersion were observed with suspension 1B and 3 when changing from 10 to 40 discs (from 0.061 to 0.060 mg/cm^2 and from 0.530 to 0.512 mg/cm^2, respectively). Besides, during coating some catalyst accumulations were observed in the mesh cover welded at both ends of the cartridge where these accumulations were more or less
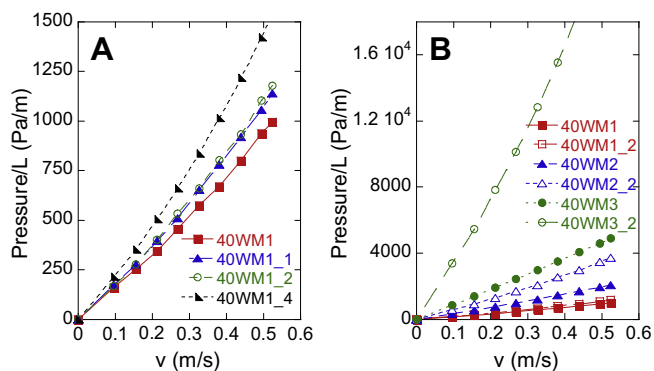
Fig. 8. Pressure drop of the wire-mesh catalyst 40WM1 coated with different amounts of catalyst (1–4 mg/cm²), using suspension 3 and three different wire meshes, 40WM1, 40WM2 and 40WM3, before (A) and after (B) the catalyst loading.
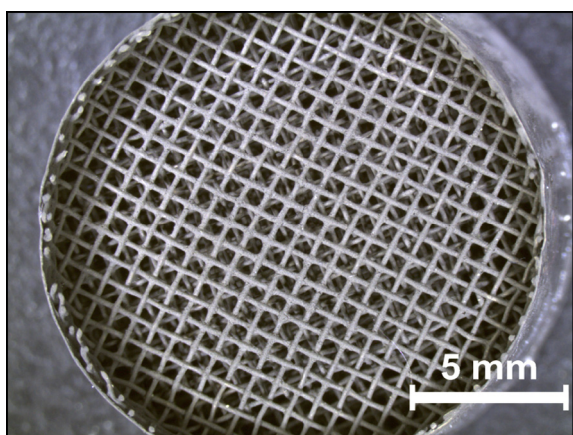

Fig. 9. Optical images of the wire-mesh structured substrate 40WM1_SUSP3/2.

Fig. 10. Characterization of the powder obtained after drying and calcination at 500 °C using suspension 3. (a) Infrared spectrum, (b) Raman spectrum and (c) X-ray diffractogram.

constant and independent of the number of discs. Therefore, when the structure contained more discs, the relative influence of these accumulations was smaller.

The SEM images of the catalytic layers obtained using the different suspensions are shown in Fig. 6. Some coating cracks were observed in the coated wire-mesh with commercial colloidal CeO_2 (suspension 1A). Nevertheless, the addition of PVA to colloidal CeO_2 (suspension 1B) resulted in an important suppression of crack formation (compare Fig. 6A and B). As a result, a better adherence was obtained, which increased from 26% to 50% at 300 °C (Table 2). Due to the observed increase in adherence (approximately 50% higher than the coating without PVA) we decided to use this additive in the other formulations. Previous studies about the coating of other structures using washcoating showed that PVA is an indispensable additive to obtain high adherence [37]. The factors that can contribute to this effect are the surface tension decrease (decrease in the capillary forces during drying that produces the cracks) and the increase in viscosity. Surprisingly, despite the increase in viscosity with respect to suspension 1A, from 11 to 15 cP, ten additional coating cycles were necessary for obtaining the same specific load with the same coating conditions (see Fig. 4), indicating that the decrease in surface tension produced by PVA is more important than the increase in viscosity from the point of view of the deposited amount. The effect of calcination temperature was also explored. Calcination can improve the cohesion of the washcoat and the metallic substrate since the small catalyst particles can coalesce forming a dense structure [26]. However,
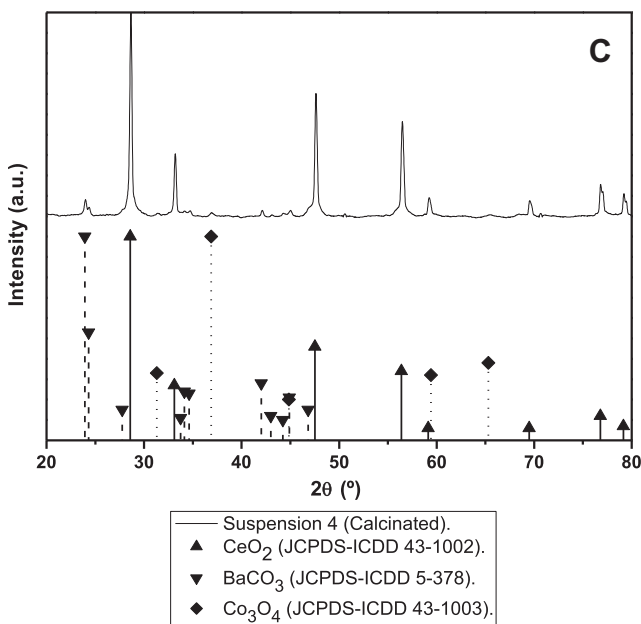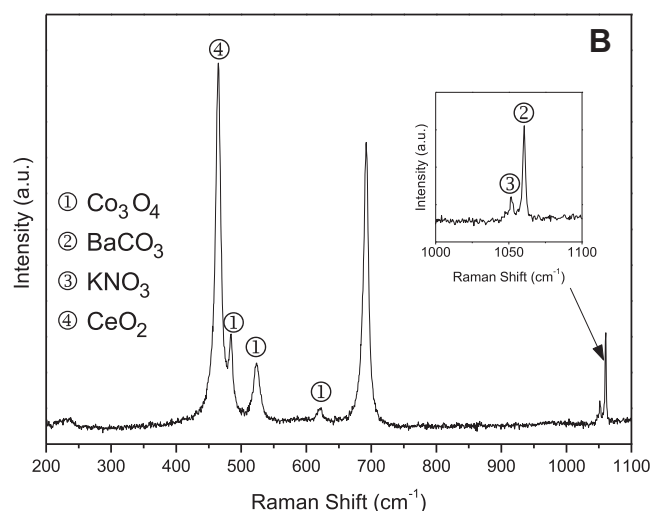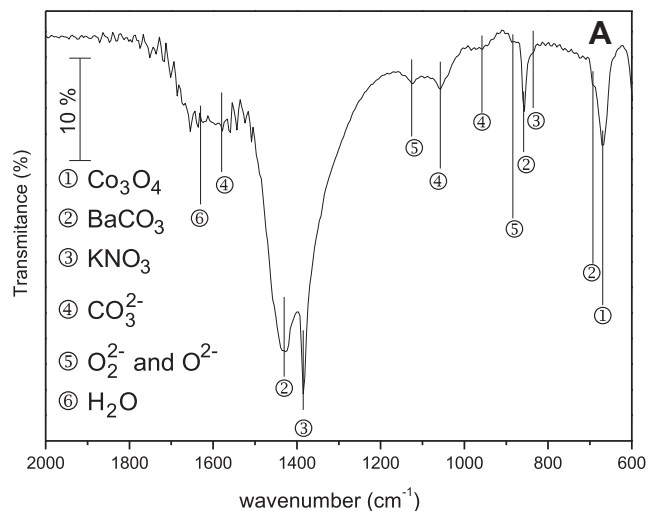
Table 3
Specific surface area of catalytic structures prepared using suspension 3 with different catalytic loading and using different wire-meshes.

Sample	Specific catalyst load (mg/cm^2)	Structure BET surface area (m^2)	Catalyst mass (mg)	Catalyst BET surface area (m^2/g)
40WM1_SUSP3/1	1	3.3	166.5	19.7
40WM1_SUSP3/2	2	4.8	269.9	17.9
40WM1_SUSP3/4	4	9.8	542.4	18.1
40WM2_SUSP3/2	2	6.8	346.2	19.6
40WM3_SUSP3/2	2	7.6	283.2	26.9
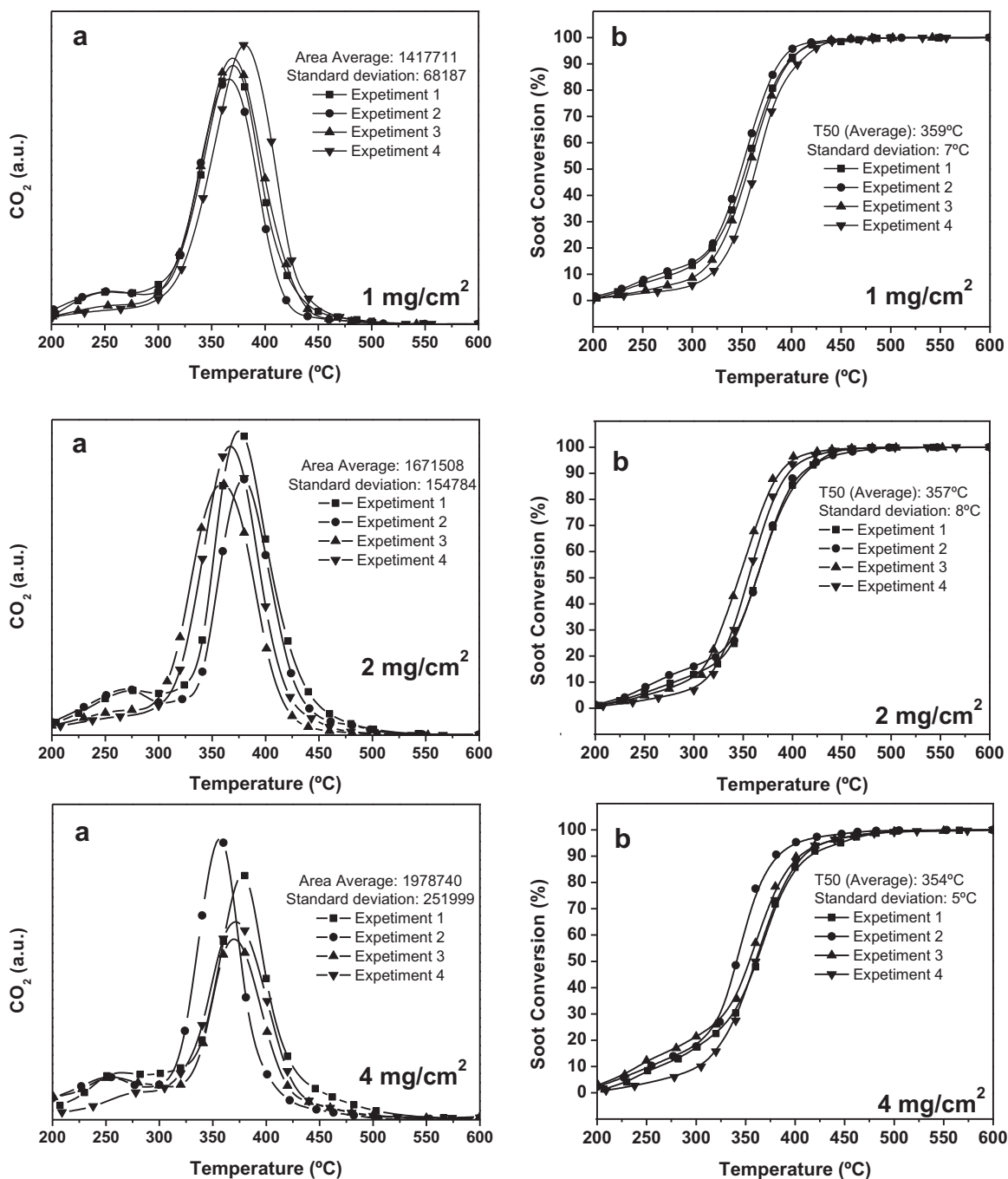
Fig. 11. Reproducibility of the catalytic test carried out with the structures made with 40WM1 loaded with 1–4 mg/cm^2 using suspension 3. Reactor feed: 18% O_2 and 0.1% NO, balance He: (a) CO_2 evolution and (b) soot conversion calculated from CO_2 data evolution.

an increase of the calcination temperature from 300 to 500 °C did not improve the adherence of CeO_2, which was a little bit higher than 70% (Table 2). The sol–gel coating strategy was discontinued

because this strategy needed too many immersions to load the desired amount of catalyst and an additional active phase impregnation step.
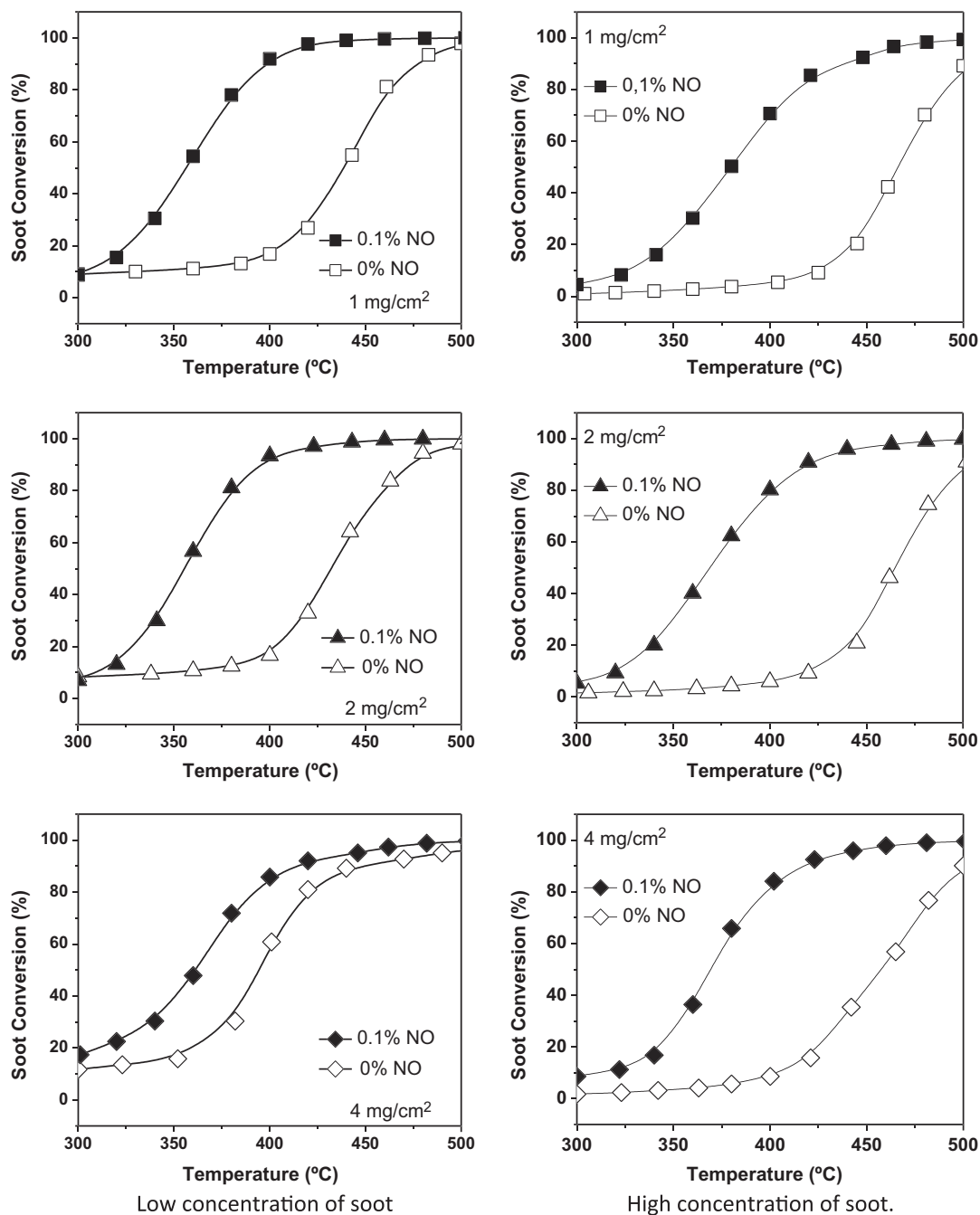
Fig. 12. Effect of NO concentration in the performance of the catalytic structure (40WM1 loaded with 1 mg/cm^2 using suspension 1), loaded either with low or high amounts of soot. O$_2$ concentration 18% (He balance).

For Suspensions 2 and 3 rough coatings were observed (Figs. 6C and D). Note the cracks developed when using suspension 2 (Fig. 6C). In the first case, the cracks were formed during the calcination of the active phase precursors at 500 °C. The adherence of this catalytic layer was poor, only 40% of the catalytic coating remained adhered to the structure wires after the ultrasonic test (Table 2). An attempt to reduce crack formation by reducing the heating rate from 5 to 1 °C/min was not successful, both samples showing the same adherence.

It can also be observed that for suspension 3 (Fig. 6D), the layer is very rough, which can be due to the big size of the particles used for the slurry preparation, morphology that has been previously

observed with other catalysts coated on structured substrates [28]. Because of the rough morphology, the adherence was excellent, higher than 90%.

Fig. 7 shows the morphologies of the coatings after the adherence test. It can be seen that near the union of two fibers, there is a zone where most of the coating is lost after the adherence test (compare Fig. 7A, B and D). These detachments are normal if we consider the structure of the wire-mesh, with wires not welded together. Then, when submitted to the ultrasonic test, an intense vibration is produced in these contact points peeling the accumulations which naturally occur at these points due to the capillary forces developed during drying. For suspension 2, which showed
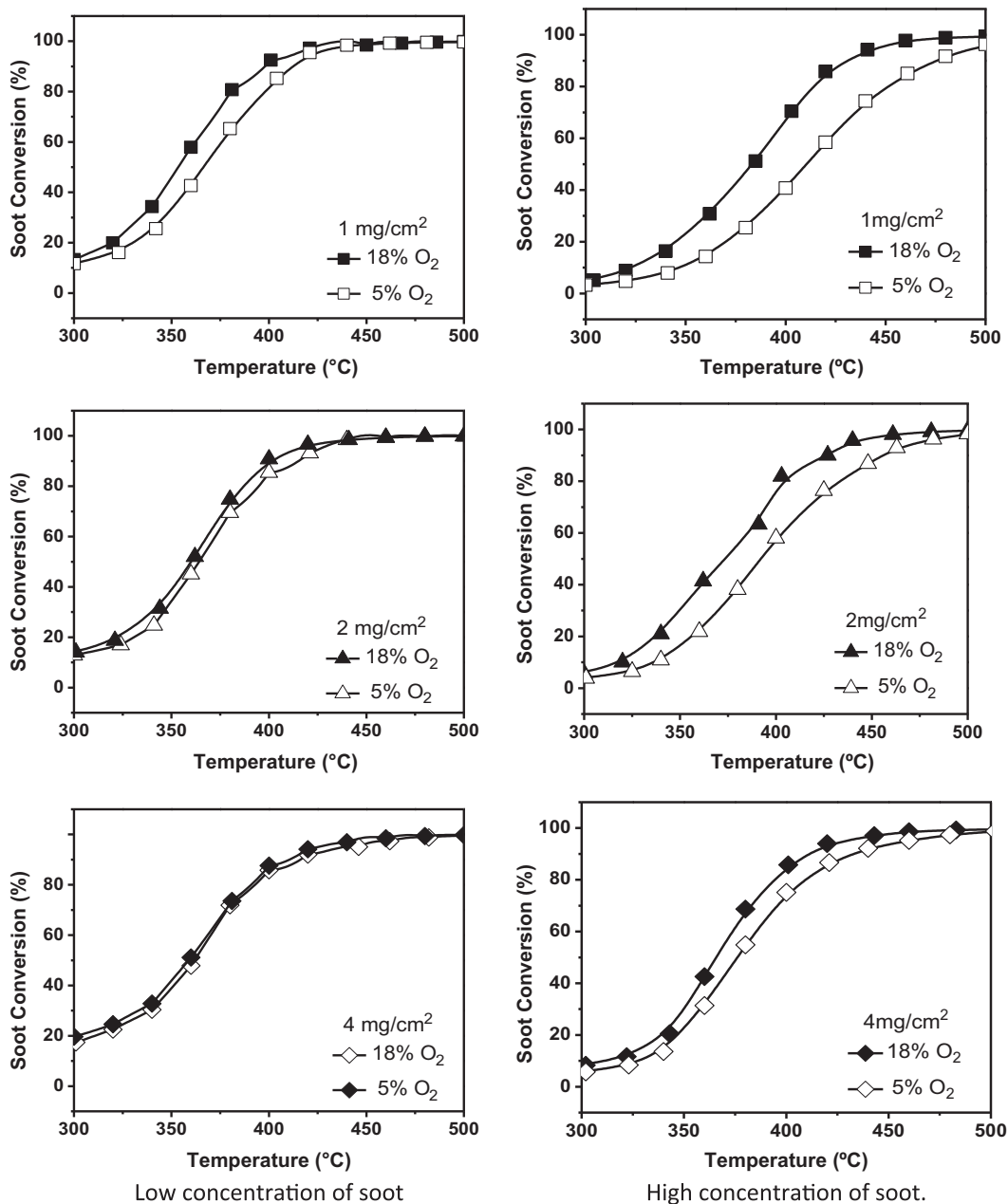
Low concentration of soot

High concentration of soot.

Fig. 13. Effect of O_2 concentration on the performance of the catalytic filter (40WM1 loaded with 1 mg/cm^2 using suspension 3), loaded either with low or high amounts of soot. NO concentration 0.1% (He balance).

the lowest adherence (only 40%), the SEM images clearly show zones where the layer is completely detached from the fibers of the wire-mesh discs (Fig. 7C).

The adherence of the catalytic layer also depends on the number of wire-mesh discs. The higher the number of wire-mesh discs (WM1), the higher the adherence of the catalytic layer. After the structure coatings, as said before, some catalyst accumulations were observed in the external part of the mesh cover welded to the cartridge, but these accumulations disappeared after the adherence test. As this amount was approximately constant and independent of the number of discs when the structure contained more discs, the effect of these accumulations on the adherence value was smaller.

On the other hand, the adherence of the catalytic layer increased with the wire-mesh opening from 58% to 95% (Table 2);

the closer the wire-mesh, the lower the adherence of the catalyst. This could be explained by the co-occurrence of several factors: the larger curvature of the surface of the wire, the greater number of intersection points of the wires and the largest accumulation plugging previously shown (Fig. 3).

In addition to adherence, the homogeneity of the catalyst film produced is a prime characteristic to evaluate the coating. SEM and optical microscopy are the techniques commonly used to check homogeneity but they require breaking and opening the structure completely. On the other side, pressure drop is a fundamental parameter in the case of mesh-structured catalysts that offer higher turbulence and radial flow than parallel channel monoliths, but at the cost of increased pressure loss. The catalyst coating on the metallic mesh can seriously increase this pressure loss if heterogeneities and plugging are produced [11]. Consequently, the measure

of the pressure drop before and after the coatings is critical in these systems, offering an average view of the coating homogeneity.

Fig. 8A presents the pressure drop of the structure made of forty discs of wire-mesh 1 (40WM1) coated with different amounts of catalyst (1–4 mg/cm²) using suspension 3. It can be seen that the pressure drop increased at increasing catalyst load, but even with the highest load, 4 mg/cm², the pressure drop increase was less than 60% at the highest gas velocities. Fig. 8B presents the pressure drop of structures made of 40 discs of the three different wire-meshes before and after loading with 2 mg/cm². From 40WM1 to 40WM3, the pressure drop increased due to the decrease in mesh opening and open frontal area. The increase in pressure drop due to the catalyst coating increased as the mesh opening decreased (from 40WM1 to 40WM3), being moderate for 40WM1 and 40WM2 but showing a dramatic increase in the case of 40WM3. This increase can be related to the partial plugging discussed before, due to the narrow mesh opening that made it difficult to eliminate the suspension excess after washcoating (Fig. 3). To obtain good coating results with 40WM3, it would be necessary to modify the method used to eliminate the suspension excess (rpm or time) or alternatively, reduce the viscosity of the catalyst suspension.

In view of the results shown above, it was decided to use catalytic structures made with 40 discs of wire mesh 1 and coated with suspension 3 in further studies of characterization and catalytic evaluation. The washcoating method with the previously synthesized catalyst on the pre-treated AISI 304 wire-mesh allows coating 40 discs without structure clogging (Fig. 9), obtaining high catalyst coating adherence with a reduced number of coating cycles and the lowest pressure drop.

3.2. Physicochemical characterization of suspension and catalytic structures

An aliquot of suspension 3 was dried and calcined at 500 °C (slurried catalyst). The powder solid thus obtained was used to check if the catalyst deposited on the metallic wire-meshes presented differences with respect to the parent catalyst.

LRS and XRD experiments were performed in order to identify the species present in the systems under study, and the results are shown in Fig. 10. The infrared spectrum of the powder obtained from suspension 3, dried and calcined, is shown in Fig. 10A. The signal corresponding to Co_3O_4 (670 cm^{-1}) [38] can be observed as well as that corresponding to $BaCO_3$ (693, 858 and 1430 cm^{-1}) [39], species that were also detected in XRD patterns (Fig. 10C). Despite the fact that KNO_3 could not be detected by XRD, it was possible to detect potassium-nitrate in the FTIR spectrum, which showed the characteristic signals at 1385 and 836 cm^{-1} [40]. Species absorbed as carbonate (958, 1058 and 1580 cm^{-1}) [41] also appear, together with water (1630 cm^{-1}). CeO_2 strongly interacts with oxygen yielding superoxide (O^{2-}) and peroxide (O_2^{2-}) species and these signals, at 1058 and 884 cm^{-1}, are clearly detected [42]. Fig. 10B shows the Raman spectrum of suspension 3 dried and calcined where it is possible to observe the signals corresponding to CeO_2 (464 cm^{-1}) [43], Co_3O_4 (485, 523, 620 and 690 cm^{-1}) [38] and the two peaks at 1052 cm^{-1} and 1059 cm^{-1}, which correspond to KNO_3 [44] and $BaCO_3$ [39], respectively.

With respect to the surface area, the uncoated calcined structures present very low values, close to the geometric surface (0.0027 m²/g). Therefore, the surface area measured for the coated catalytic structure corresponds to that of the catalytic layer. For the Co, Ba, K/CeO₂ powder catalyst used to prepare suspension 3, the surface area was 9.7 m²/g. This powder catalyst was prepared from commercial CeO₂, which explains this low surface area value. However, when suspension 3 was dried and calcined, the surface area was 27.7 m²/g. This higher value is due to the colloidal ceria (Nyacol®) used as additive in suspension 3 because this ceria

presented 130 m²/g after drying and calcination. Table 3 shows the BET surface area of the coatings supported on the structured substrates. It can be observed that a similar surface area was obtained in all the samples except for the structure prepared with WM3 that presented a slightly higher surface area of the coating (26.9 m²/g) similar to that of the suspension dried and calcined (27.7 m²/g).

3.3. Catalytic combustion of diesel soot on coated wire-mesh structures. TPO experiments

These experiments were performed using structures made with 40 discs of wire-mesh 1 (40WM1). Fig. 11 shows four catalytic tests carried out with structures loaded with 1 mg/cm² using suspension 3. It can be observed that measurements are reproducible, showing very similar temperatures for 50% of conversion (Fig. 11b). The amount of soot burnt is proportional to the area under the TPO curve (Fig. 11a), which is similar in the four experiments. These results confirm that the method selected for the impregnation of soot in the structure is adequate for the measurement of the catalytic performance.

Figs. 12 and 13 show the results of the catalytic tests performed for the structures 40WM1 loaded with 1 mg/cm², 2 mg/cm² and 4 mg/cm² of suspension 3. In this series, different values of NO and O₂ concentrations and different amounts of soot loaded in the structure were evaluated.

In Fig. 12, the promoting effect of NO is clearly observable. As a matter of fact, the soot conversions occur at lower temperatures when NO is present in the feed. This is not surprising, as it is well known that NO in the presence of O₂ forms NO₂, which is more oxidant than O₂ [45]. Table 4 presents the temperature values for 10%, 50% and 90% of soot conversion corresponding to Fig. 12. It can be seen that, when NO is fed, the temperature for 50% of soot combustion is only slightly decreased by the increased amount of soot loaded in the structure. However, in the absence of NO, higher amounts of soot are more detrimental for the performance of the structure and it is not completely burnt up to 500 °C. This can be ascribed to the contact between soot, O₂ and the catalyst, which is poorer for higher soot loadings but when NO is fed, the direct reaction between NO₂ and soot helps to overcome the contact effect. This phenomenon has also been previously reported for powder catalysts [36,46–48].

Table 4
Temperatures corresponding to 10% of soot conversion (T10), 50% of conversion (T50) and 90% of conversion (T90). Data obtained from Figs. 11 and 12.

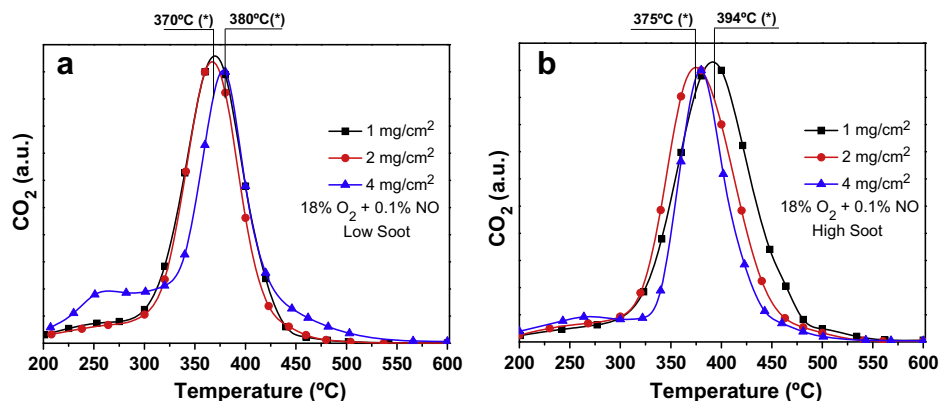| Catalyst load (mg/cm²)	O₂ (%)	NO (%)	Soot amount		Temperature (°C)		
			Low	High	T_{10}	T_{50}	T_{90}
1	18	0.1	√		302	356	398
1	18	0	√		329	438	478
1	5	0.1	√		288	366	412
1	18	0.1		√	359	379	439
1	18	0		√	424	366	505
1	5	0.1		√	346	410	475
2	18	0.1	√		308	355	395
2	18	0	√		347	432	473
2	5	0.1	√		280	364	412
2	18	0.1		√	318	368	464
2	18	0		√	419	464	503
2	5	0.1		√	327	392	438
4	18	0.1	√		262	361	415
4	18	0	√		278	394	450
4	5	0.1	√		263	361	413
4	18	0.1		√	310	369	417
4	18	0		√	403	457	503
4	5	0.1		√	335	375	456

Fig. 14. CO_2 evolution with structures made with 40WM1 loaded with 1–4 mg/cm^2 using suspension 3. Reactor feed: 18% O_2 and 0.1% NO, balance He. Low soot load (a) and high soot load (b). ($*$) Temperature of the maximum combustion rate.

Fig. 13 shows the effect of the O_2 concentration on the catalytic performance of the structures. It is clearly observable that the decrease in O_2 concentration slightly decreases the performance. Interestingly, when increasing the amount of catalyst coated in the structure, the difference between the temperatures of 50% of conversion becomes smaller, effect that is probably due to the CeO_2 surface oxygen availability [49].

The catalytic structures presented in this work have shown to be interesting systems to be applied for the abatement of diesel soot. The average temperature of diesel exhaust gases, when passed through the particulate structures, is close to 400 °C, which is higher than the temperature of maximum combustion rates obtained in this work. Those are close to 375 °C (Fig. 14a) when a low amount of soot is deposited on the catalyst, and to 385 °C (Fig. 14b) for higher soot loadings. The low pressure drop and the good catalytic performances they exhibit, merit further studies in order to check the particle retention capacity of these structures. In this sense, wire-mesh structures would act as deep-bed filters, where a good penetration/dispersion of particulate inside the trap matrix is expected, thus allowing constant collection efficiency. The study here reported, in which the catalytic coverage of wire meshes and their performances towards the soot combustion reaction is analyzed, constitutes the first step for developing self-regenerating diesel soot wire-mesh filters.

4. Conclusions

The viability of the use of wire-mesh structures for the catalytic combustion of diesel soot has been shown in this study.

- First of all, information about the key parameters of the design and fabrication of stacked wire-mesh structures has been given.
- The most relevant conclusion of this study is that the Co, Ba, K/CeO$_2$ catalyst was successfully washcoated on metallic wire-mesh structures using different washcoating strategies. To use commercial colloidal ceria (suspension 1A and 1B), it is necessary to incorporate PVA to avoid coating cracks. However, despite having an excellent adherence, too many coatings were necessary to obtain a desired catalyst load on the structure. Taking into account that additional preparation steps (impregnation of active phases) would be necessary, this strategy was abandoned. The all-in-one suspension strategy (suspension 2) produced coatings with big cracks during the calcination that were poorly adhesive. On the contrary, the slurry with a previously prepared catalyst (suspension 3) presented a homogenous and very adherent catalytic layer which needed very few coatings, therefore being considered the most interesting strategy.

- On the other hand, the wire-mesh geometry (number of discs and wire-mesh type) influenced the adherence of the catalyst directly.
- Finally, the catalytic structures showed a better activity for the abatement of diesel soot than those present in normal diesel engine exhausts.
- Although further research is necessary to check the filtration efficiencies of the structures here developed, our own results as well as those reported by others [10,14] encourage us to deepen the study of these systems for the potential application as diesel soot filters.

References

[1] T.V. Johnson, SAE Int. J. Fuels Lubr. (October) 98 (2009) 1–12.
[2] D. Fino, Sci. Technol. Adv. Mater. 8 (2007) 93–100.
[3] M.E. Gálvez, S. Ascaso, I. Tobías, R. Moliner, M.J. Lázaro, Catal. Today 191 (2012) 96–105.
[4] B.A.A.L. Van Setten, M. Makkee, J.A. Moulijn, Catal. Rev. 43 (2001) 489.
[5] E.D. Banús, V.G. Milt, E.E. Miró, M.A. Ulla, Appl. Catal B: Environ. 132–133 (2013) 479–786.
[6] J.P.A. Neeft, M. Makkee, J.A. Moulijn, Fuel Process. Technol. 47 (1996) 1–69.
[7] W.M. Carty, P.W. Lednor, Curr. Opin. Solid State Mater. Sci. 1 (1996) 88.
[8] S. Bensaid, N. Russo, Catal. Today 176 (2011) 417–423.
[9] E. Vanhaecke, C. Pham-Huu, D. Edouard, Catal. Today 189 (2012) 101–110.
[10] E.D. Banús, V.G. Milt, E.E. Miró, M.A. Ulla, Appl. Catal. A: Gen. 379 (2010) 95–104.
[11] A.F. Ahlström-Silversand, C.U. Ingemar-Odenbrand, Appl. Catal. A: Gen. 153 (1997) 177–201.
[12] Y. Matatov-Meytal, M. Sheintuch, Appl. Catal. A: Gen. 231 (2002) 1–16.
[13] P. Doggali, H. Kusaba, S. Rayalu, Y. Teraoka, N. Labhsetwar, Top. Catal. 56 (2013) 457–461.
[14] H.O. Handerberg, SAE paper 870011, 1987.
[15] K.-S. Chung, Z. Jiang, B.-S. Gill, J.S. Chung, Appl. Catal. A: Gen. 237 (2002) 81–89.
[16] G. Marbán, A. López, I. López, T. Valdés-Solís, Appl. Catal. B: Environ. 99 (2010) 257–264.
[17] K.S. Yang, J.S. Choi, J.S. Chung, Catal. Today 97 (2004) 159–165.
[18] A.E.W. Beers, T.A. Nijhuis, N. Aalders, F. Kapteijn, J.A. Moulijn, Appl. Catal. A: Gen. 243 (2003) 237–250.
[19] A.F. Ahlström-Silversand, C.U. Ingemar-Odenbrand, Chem. Eng. J. 73 (1999) 205–216.
[20] K.S. Yang, G. Mul, J.S. Choi, J.A. Moulijn, J.S. Chung, Appl. Catal. A: Gen. 313 (2006) 86–93.

[21] C.N. Satterfield, Heterogeneous Catalysis in Industrial Practice, second ed., MaGraw-Hill, New York, 1991.
[22] P. Ávila, M. Montes, E.E. Miró, Chem. Eng. J. 109 (2005) 11–36.
[23] V. Meille, Appl. Catal. A: Gen. 315 (2006) 1–17.
[24] M.F.M. Zwinkels, S.C. Jaras, P.G. Menon, T.A. Griffin, Catal. Rev. Sci. Eng. 35 (1993) 319–358.
[25] W.F. Maier, J.W.A. Schalangen, Catal. Today 17 (1993) 225–233.
[26] H. Sun, X. Quan, S. Chen, H. Zhao, Y. Zhao, Appl. Surf. Sci. 253 (2007) 3303–3310.
[27] K.D. Deeng, A.R. Mohamed, S. Bhatia, Chem. Eng. J. 103 (2004) 147–157.
[28] C. Agrafiotis, A. Tsetsekou, J. Europ. Ceram. Soc. 20 (2000) 815–824.
[29] O. Sanz, L.C. Almeida, J.M. Zamaro, M.A. Ulla, E.E. Miró, M. Montes, Appl. Catal. B: Environ. 78 (2008) 166–175.
[30] L.M. Martínez, O. Sanz, M.I. Domínguez, M.A. Centeno, J.A. Odriozola, Chem. Eng. J. 148 (2009) 191–200.
[31] J.P. Bortolozzi, E.D. Banús, V.G. Milt, L.B. Gutierrez, M.A. Ulla, Appl. Surf. Sci. 257 (2010) 495–502.
[32] V.G. Milt, C.A. Querini, E.E. Miró, M.A. Ulla, J. Catal. 220 (2003) 424–432.
[33] S. Vallar, D. Houivet, J. El Fallah, D. Kervadec, J.M. Haussonne, J. Eur. Ceram. Soc. 19 (1999) 1017–1021.
[34] S. Yasaki, Y. Yoshino, K. Ihara, K. Ohkubo, US Patent 5,208,206, 1993.
[35] B.A.A.L. van Setten, J.M. Schouten, M. Makkee, J.A. Moulijn, Appl. Catal. B: Environ. 28 (2000) 253–257.
[36] V.G. Milt, E.D. Banús, M.A. Ulla, E.E. Miró, Catal. Today 133–135 (2008) 435–440.
[37] O. Sanz, F.J. Echave, F. Romero-Sarria, J.A. Odriozola, M. Montes, Renewable Hydrogen Technologies (2013) 201–224.
[38] L.-H. Ai, J. Jiang, Powder Tech. 195 (2009) 11–14.
[39] P. Pasierb, S. Komornicki, M. Rokita, M. Rekas, J. Mol. Structure 596 (2001) 151–156.
[40] F.A. Miller, C.H. Wilkins, Anal. Chem. 24 (1952) 1253–1294.
[41] Anatoli Davydov, N.T. Sheppard (Eds.), Molecular Spectroscopy of Oxide Catalyst Surfaces, John Wiley & Sons Ltd., 2003. p. 135.
[42] C. Binet, M. Daturi, J.C. Lavalley, Catal. Today 50 (1999) 207–225.
[43] M.P. Woods, P. Gawade, B. Tan, U.S. Ozkan, Appl. Catal B: Environ. 97 (2010) 28–35.
[44] R. Murugan, P.J. Huang, A. Ghule, H. Chang, Thermochim. Acta 346 (2000) 83–90.
[45] A. Setiabudi, B.A.A.L. van Setten, M. Makkee, J.A. Moulijn, Appl. Catal. B: Environ. 35 (2002) 159–166.
[46] V.G. Milt, E.D. Banús, E.E. Miró, M. Yates, J.C. Martín, S.B. Rasmussen, P. Ávila, Chem. Eng. J. 157 (2010) 530–538.
[47] Z. Li, M. Meng, Q. Li, Y. Xie, T. Ho, J. Zhang, Chem. Eng. J. 164 (2010) 98–105.
[48] F. Lin, X. Wu, S. Liu, D. Weng, Y. Huang, Chem. Eng. J. 226 (2013) 105–112.
[49] E.E. Miró, F. Ravelli, M.A. Ulla, L.M. Cornaglia, C.A. Querini, Catal. Today 53 (1999) 631–638.